Water-Induced Self-Assembling of Solvent-Sensitive Block Copolymer

Chieko Fuse,[†] Satoshi Okabe,[†] Shinji Sugihara,[‡,§] Sadahito Aoshima,[‡] and Mitsuhiro Shibayama*[,†]

Neutron Science Laboratory, Institute for Solid State Physics, The University of Tokyo, Tokai, Ibaraki, 319-1106, Japan, and Department of Macromolecular Science, Graduate School of Science, Osaka University, Toyonaka, Osaka 560-0043, Japan

Received March 6, 2004; Revised Manuscript Received June 3, 2004

ABSTRACT: The microphase separation of a solvent-sensitive self-assembling block copolymer, poly(2-phenoxyethyl vinyl ether)-*block*-poly(2-methoxyethyl vinyl ether) (pPhOVE−pMOVE), in acetone/water mixture was investigated by small-angle neutron scattering (SANS). Acetone solutions of pPhOVE−pMOVE undergo tremendous viscosity thickening by adding small amount of water as a result of formation of spherical domains highly ordered in a body-centered cubic (bcc) lattice with interdomain entanglements of tethered chains. A contrast variation SANS allowed us to elucidate the architecture consisting of gathered pPhOVE domains with tethered pMOVE chains spread in the matrix. The structure evolution of this "water-induced microphase separation" was compared with that of heat-induced microphase separation. It was found that the former is an amplification process of concentration fluctuations like spinodal decomposition and the latter is analogous to a nucleation-and-growth mechanism.

Introduction

Block copolymers have been extensively investigated and widely used in application in the past four decades because of their unique features of the capability of microphase separation. Molau[1] classified the morphologies of A−B type diblock copolymers, i.e., a polymer consisting of two unlike A and B block chains chemically cross-linked to each other, as a function of the composition of A. Thermodynamic theories of block copolymers predict the relationships between the molecular length and the size of the microphase separation and between the morphology and the composition.[2−5] Studies on temperature and concentration dependence of the microphase separation disclosed the presence of order−disorder transitions of block copolymers, which is analogous to the order−disorder transition of binary fluids and magnetic matter.[6,7] Block copolymers in semidilute and concentrated solutions exhibit more attractive phase behaviors and rheological properties than in bulk because of another degree of freedom, i.e., polymer concentration. Typical examples are polystyrene−polydiene block copolymers[8−12] and poly(oxyethylene)-containing block copolymers in aqueous solutions.[13−16]

Aoshima et al. succeeded in synthesizing a series of stimuli-responsive block copolymers with pendant alcohol[17,18] and oxyethylene.[19−22] Because of a narrow molecular weight distribution, a sharp transition in turbidity as well as in viscosity with respect to temperature was achieved. Among various combinations of block chains, it was found that poly(2-phenoxyethyl vinyl ether)-*block*-poly(2-methoxyethyl vinyl ether) (pPhOVE−pMOVE) is very sensitive to the choice of solvents.[21] The chemical structure of pPhOVE−pMOVE is shown in Chart 1. This is due to the difference in solubility of the constituent homopolymers, pPhOVE and pMOVE, to solvents as shown in Table 1. The circles and crosses in Table 1 respectively mean that the polymers are soluble and insoluble to the solvents at room temperature. pPhOVE is soluble to nonpolar solvents while pMOVE to polar solvents, indicating that they have hydrophobic and hydrophilic nature, respectively. As a result, the pPhOVE−pMOVE behaves as a polyampholyte, like a "polymer soap". In this work, we chose acetone and water as a common and a selective solvent, respectively. Interestingly enough, it was revealed that the viscosity of pPhOVE−pMOVE acetone solutions increased abruptly but continuously by adding water (Figure 1). In addition, the system underwent a sol−gel transition by addition of water, where the gel phase was determined by tilting-a-tube method. Figure 2 shows a triangle phase diagram of the pPhOVE−pMOVE/acetone/water solutions at 30 °C. The horizontal axis is the polymer concentration, C, and the other axis is the solvent composition, f_w. Here we define the

Chart 1

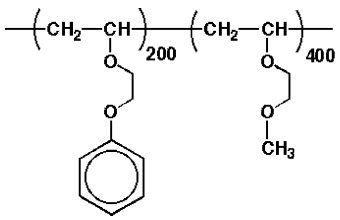

Table 1. Solubility Characteristics of the Homopolymers Composing Block Segments of pPhOVE−pMOVE at Room Temperature.

solvent	pPhOVE	pMOVE
water	×	○
methanol	×	○
ethanol	×	○
n-hexane	×	×
heptane	×	×
cyclohexane	×	○
toluene	○	○
acetone	○	○

[a] Key: circles: soluble, crosses: insoluble.

* To whom correspondence should be addressed.
[†] The University of Tokyo.
[‡] Osaka University.
[§] Present address: Department of Applied Chemistry and Biotechnology, Faculty of Engineering, University of Fukui, Bunkyo, Fukui 910-8507, Japan.

10.1021/ma0495442 CCC: $27.50
Published on Web 08/28/2004

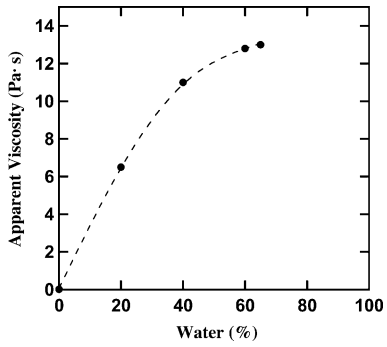

Figure 1. Apparent viscosity (shear rate = 10 s^{-1}) of pPhOVE−pMOVE gels with different solvent compositions (acetone/water).

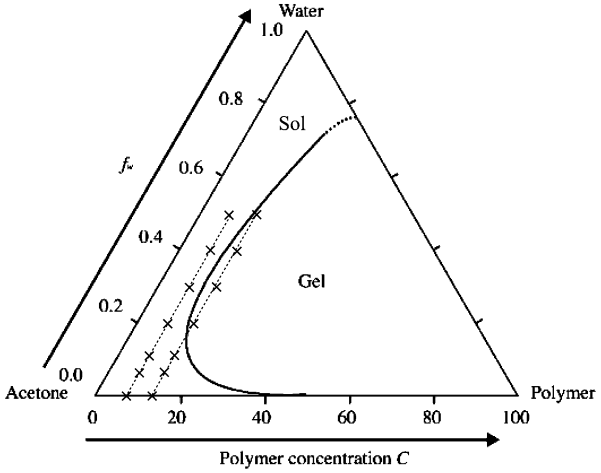

Figure 2. Triangle phase diagram for pPhOVE−pMOVE/acetone/water at 30 °C.

value C and f_w as the weight percentage of the polymer in solution and the weight fraction of water in the mixed acetone/water solvent, respectively. The phase diagram is divided to two regions, i.e., solution and gel. In this study, we employed small-angle neutron scattering (SANS) to investigate the microphase-separated structures of pPhOVE−pMOVE solutions and gels in various solvent compositions and polymer concentrations.

Experimental Section

Samples. pPhOVE−pMOVE with a narrow molecular weight distribution (M_n = 73.7 × 10^3, M_w / M_n = 1.18) was synthesized by living cationic polymerization consisting of 200 and 400 monomer units for pPhOVE and pMOVE, respectively.[21] The number-average molecular weights (M_n) of pPhOVE and pMOVE are 32.8 × 10^3 and 40.9 × 10^3, respectively. Hence, the molecular weight ratio of pPhOVE to the total block copolymer is 0.445. The corresponding homopolymer pPhOVE was polymerized in toluene at 0 °C in the presence of ethyl acetate with $Et_{1.5}AlCl_{1.5}$ under dried nitrogen atmosphere. Without an induction phase, the polymerization proceeded smoothly to reach 100% conversion, and a monotonic increase in number-average molecular weight with monomer conversion was observed, indicating living polymerization. After the polymerization of PhOVE (20.5 h) was completed, the second monomer, MOVE in neat form, was added into the system. The sequential living cationic copolymerization, after sufficient conversion time, namely 3.0 h (total 23.5 h), was quenched with methanol containing a small amount of aqueous ammonia solution (0.3 wt %) and washed with 0.6 N hydrochloric acid to remove the initiator residues and to neutralize the system. The synthesized pPhOVE−pMOVE was collected by evaporation of the solvents under reduced pressure.

Gel and solution samples of pPhOVE−pMOVE were prepared by first dissolving the polymer into acetone and then adding water to make series of samples with the same polymer concentration but with different water contents. Before and after addition of water, all the samples were shaken for 30 min for complete dissolution. For C = 12 wt % samples, we heated the samples with a water bath at 45°C after adding water to avoid nonuniform solvation. For all the SANS experiments except for the contrast variation experiment, deuterated acetone (99.9% deuteration) and deuterium oxide (99.9% deuteration) were used as the solvents in order to obtain enough scattering contrast between the polymer and the solvents.

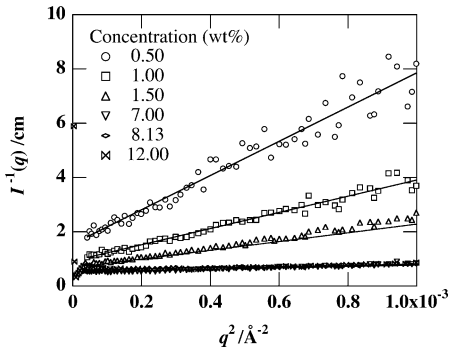

Figure 3. Ornstein−Zernike plots of pPhOVE−pMOVE in acetone-*d* solutions observed at 20 °C.

SANS. All the SANS data in this paper were acquired using a SANS-U spectrometer, Institute for Solid State Physics, the University of Tokyo. A flux of cold neutrons was obtained from the JRR-3M research reactor of Japan Atomic Energy Research Institute, Tokai, Ibaraki, Japan. The cold neutron beam was monochromatized with a velocity selector to 7.0 Å with 13% wavelength distribution. The temperature of the samples was controlled with a water-circulating bath (NESLAB RTE-111M) with a precision of ±0.1 °C. Samples in quartz cells of 2 or 4 mm thickness were measured for sufficient period of time depending on the transmission and the scattering power of the samples to gain enough statistics, namely 10−120 min. The scattered intensity profiles obtained by the two-dimensional ^{3}He detector at the sample-to-detector distances (SDD) = 2 and 8 m were circularly averaged and corrected for transmission, cell scattering, and incoherent backgrounds, and then were combined to a master scattering function to cover a wide range of the scattering vector, q, i.e., 0.006 ≤ q ≤ 0.15 Å^{-1}. Thus, corrected scattering intensity was scaled to the absolute scattering intensity, $I(q)$, i.e., the differential cross-section, with the incoherent scattering intensity from a Lupolen (polyethylene) secondary standard sample.

Results and Discussion

1. Acetone Solutions. In acetone solutions, the scattering intensity functions, $I(q)$s, were relatively low and was a monotonic decreasing function with q. According to the following equation,[6] the correlation length, ξ, was evaluated.

$$I_{OZ}(q) = \frac{I_{OZ}(0)}{1 + \xi^2 q^2} \quad (1)$$

Figure 3 shows Ornstein−Zernike (OZ) plots ($I^{-1}(q)$ vs q^2) of the pPhOVE−pMOVE in deuterated acetone (d−acetone) solutions in the concentration regimes of C = 0.5 wt % to 12 wt %. The SANS data seem to be well fitted to OZ functions. Figure 4 shows the variation of ξ with C. The dashed line is guide for the eye. For $C \geq$ 7 wt %, the following relation was obtained $\xi \sim C^{-0.58}$. Hence, it is deduced that the pPhOVE−pMOVE polymer chains are somewhat in an expanded state as in a good solvent, and chain overlapping takes place for at least $C \geq$ 7 wt %.

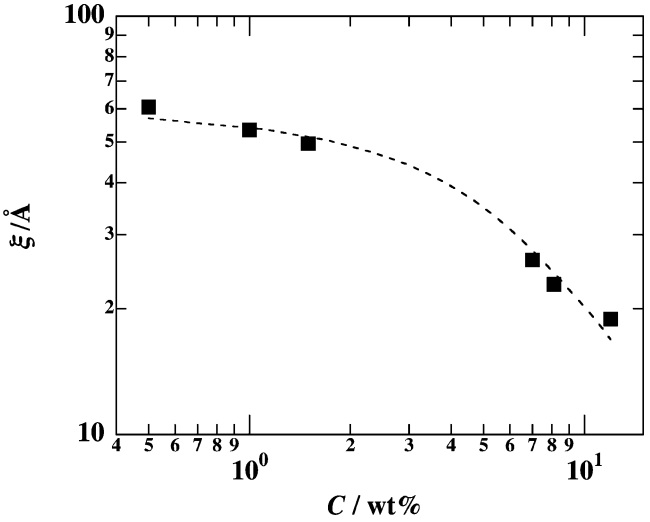

Figure 4. Variation of ξ with C for pPhOVE−pMOVE acetone solutions observed at 20 °C.

2. Microphase Separation Transition Accompanying the Sol—Gel Transition. In Figure 5, we show the scattering intensity profiles, $I(q)$s, for pPhOVE−pMOVE solutions at (a) $C = 7$ wt % and (b) $C = 12$ wt %, with different solvent compositions, f_ws. In the case of acetone solution, i.e., $f_w = 0$, $I(q)$ is well described by eq 1 as discussed above. However, by addition of small amount of water, e.g., $f_w = 0.05$, a broad peak appeared at $q \approx 0.012$ Å^{-1} for $C = 7$ wt % and at $q \approx 0.015$ Å^{-1} for $C = 12$ wt %. The peaks evolved with increasing water content, and then new peaks appeared at a lower q region as shown by the thick arrows. As a result, $I(q)$ increased dramatically by a hundred times in the intensity with distinct peaks in the lower q region. All of these peaks are more clearly seen in the samples of $C = 12$ wt %, where multiple peaks at low q's indicate the presence of well-ordered structure as will be discussed later.

These peaks in Figure 5 suggest emergence of a nanoorder assembled structure in the polymer solution. The peaks of $I(q)$s at higher q values ($q > 0.03$ Å^{-1}) shown by the thin arrows indicate the existence of spherical domains. On the other hand, the peaks at lower q value ($q < 0.03$ Å^{-1}) shown by thick arrows indicate a highly ordered arrangement of the domains. From the relative positions of the first, second, and third peaks of $C = 12$ wt %, i.e., 1, $\sqrt{2}$, $\sqrt{3}$, we assigned this ordered structure to be a body-centered cubic (bcc). It should be also noted here that the appearance of these peaks is very different from the case of heat-induced microphase separation observed by Shibayama et al.,[23] where the peaks related to spherical micelles appear first followed by emergence of interference peaks. Here, we will carry out the fitting of these profiles in the next section.

3. Quantitative Analysis of the Microphase-Separated Structure. With the same method employed in the previous paper,[23] we performed fittings of the SANS profiles using the three-dimensional paracrystal theory.[24−27] The scattering intensity function consists of two parts, namely the form factor for noninterfering spherical particles, $P(q)$, and the lattice factor, $Z(q)$. The fitting function is the multiplication of the two functions in addition to the contribution from scattering of the matrix and is expressed as

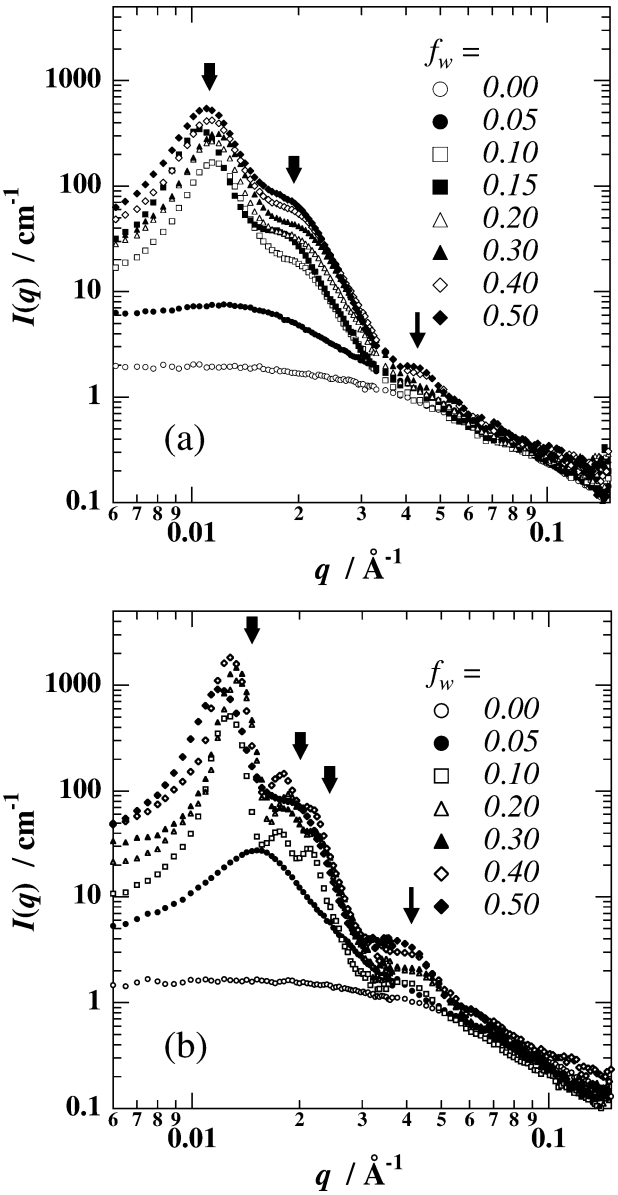

Figure 5. Scattering intensity functions, $I(q)$s, for (a) 7 and (b) 12 wt % pPhOVE−pMOVE in acetone/water with different water weight fractions, f_ws.

$$I(q) = P(q)Z(q) + I_{OZ}(q) \tag{2}$$

where the first and second terms of the RHS represent the scattered intensities for spherical domains and for semidilute solutions, i.e., the OZ function, respectively.

$$P(q) = nV^2\Delta\rho^2\Phi^2(qR) \tag{3}$$

$$\Phi(qR) = \frac{3[\sin(qR) - qR \times \cos(qR)]}{(qR)^3} \equiv \sqrt{\frac{\pi}{2}}\frac{J_{3/2}(qR)}{(qR)^{3/2}} \tag{4}$$

where n is the number density of the spheres, $\Delta\rho^2$ is the square of the difference in the scattering length densities of a spherical particle and a matrix, R is the radius of the sphere, and V is the volume of the sphere. $Z(q)$ is obtained by multiplying $Z_k(q)$ for $k = 1$, 2, and 3, and then integrating for all the possible orientations (k is the axis number in the three-dimensional rectangular coordinate).

$$Z_k(q) = \frac{1 - |F(q)|^2}{1 - 2|F(q)|\cos(\vec{a}_k \cdot \vec{q}) + |F(q)|^2} \quad (5)$$

$$|F(q)| = \exp\left[-\frac{1}{2}\frac{\Delta a^2}{a^2}\{(\vec{a}_1 \cdot \vec{q})^2 + (\vec{a}_2 \cdot \vec{q})^2 + (\vec{a}_3 \cdot \vec{q})^2\}\right] \quad (6)$$

$\vec{a}_k$'s are the unit vectors in the directions of $k = 1, 2, 3$, respectively. Δa is the distortion from the ideal lattice point, assuming the isotropic distortions.

For the size distribution of spheres, a weighting function, $W_R(R)$, was introduced and assumed to be a Gaussian function given by

$$W_R(R) \sim \exp\left[-\frac{(R - \langle R \rangle)^2}{2\Delta R^2}\right] \quad (7)$$

where $\langle R \rangle$ is the average radius of the sphere and ΔR is the deviations. Hence eq 3 has to be rewritten to[28]

$$P_R(q) = \langle n \rangle \Delta\rho^2 \frac{\int W(R) V^2(R) \Phi^2(qR)\, dR}{\int W(R)\, dR} \quad (8)$$

Here, $\langle n \rangle$ is the average number of spheres in a unit volume and is given by

$$\langle n \rangle = \frac{2}{\langle a \rangle^3} \quad (9)$$

In addition, we evaluate the instrumental smearing effect[23] with the resolution function, which is assumed to be a Gaussian distribution.

$$W_{pin}(q) \sim \exp\left[-\frac{q^2}{2\sigma_{pin}^2}\right], \quad \sigma_{pin} = \mathrm{FWHM}/2\sqrt{2 \ln 2} \quad (10)$$

Here, σ_{pin} and FWHM are the standard deviation and the full-width at half-maximum of the incident beam. The value of FWHM at SDD = 8m of the SANS−U was evaluated to be 1.35×10^{-3} Å^{-1}. For the fitting of the obtained profiles, we used the smeared intensity, $I_{fit}(q)$, given by

$$I_{fit}(q) = I(q)^* W_{pin}(q) = \int I(q') W_{pin}(q - q')\, dq' \quad (11)$$

where the asterisk in eq 11 denotes the convolution product. Further explanations of the fitting function are available on previous papers.[23,27] In the higher q region, i.e., $q \geq 0.05$ Å^{-1}, it was found that the profiles did not follow Porod's rule, and $I(q)$ decreased with a power of −2 instead of −4. This q dependence of $I(q)$ indicates that the spherical domains are embedded in a semidilute polymer solution.

In Figure 6, we show an example of the results of the fitting for $f_w = 0.1$. The fitted curve designated by the solid line reproduced the observed scattering function quite well. The two-dot-chain line indicates the contribution of $I_{OZ}(q)$, from which the correlation length, ξ, was evaluated to be 19 Å. This value is in good agreement with that observed in 12 wt % acetone solution of pPhOVE−pMOVE. Hence, the model, spherical domains embedded in a polymer solution, seems to be valid. From the fitting for $q \leq 0.05$Å^{-1}, we obtained the structure parameters, i.e., the size of the microdomains and the lattice spacing, $\langle R \rangle$ and $\langle a \rangle$, their relative deviations, $\Delta R/\langle R \rangle$ and $\Delta a/\langle a \rangle$. We carried out the same fitting for the other profiles showing distinct peaks.

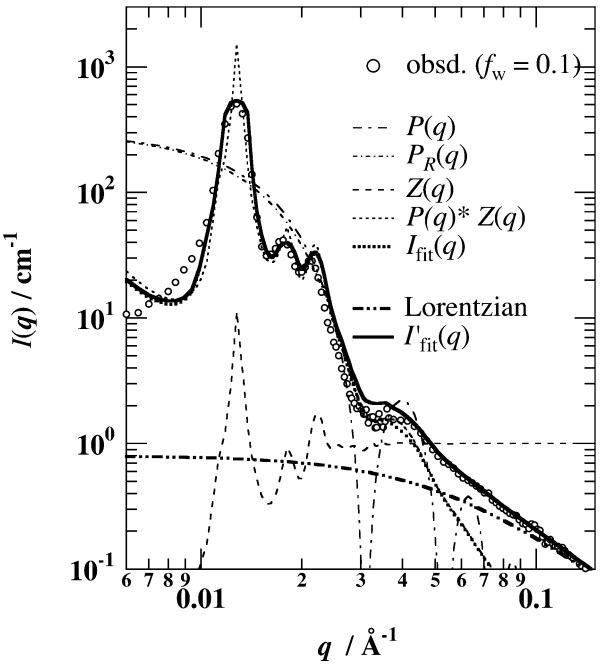

Figure 6. Result of curve fitting of $I(q)$ for microphase-separated pPhOVE−pMOVE for $C = 12$ wt % and $f_w = 0.1$.

The variations of these structure parameters with f_w are shown in Figure 7.

As shown in the figure, the radius of the spherical domains, $\langle R \rangle$, seems to be an increasing function of f_w, while that of $C = 7$ wt % is somewhat scattered. The larger in C, the larger in $\langle R \rangle$. This is due to an increase in the Flory interaction parameter, χ, by increasing C or f_w. The radius of spherical microdomains in a good solvent is an increasing function of χ as discussed elsewhere.[10] The lattice size, $\langle a \rangle$, also tends to increase with increase in f_w, and $\langle a \rangle = 790$ and 650 Å in average for $C = 7$ wt % and 12 wt %, respectively. Thermodynamically, the value of $\langle a \rangle$ is determined by minimizing density fluctuations of the solution/gels in the presence of dispersing domains. As C increases, $\langle R \rangle$ increases and $\langle a \rangle$ decreases as in the case of other block copolymers in selective solvents.[11] The variations of (c) $\Delta R/\langle R \rangle$ and (d) $\Delta a/\langle a \rangle$ were also evaluated owing to the curve fitting. The value of $\Delta R/\langle R \rangle$ is, in general, decreasing functions with increase in f_w and C, suggesting a more uniform spherical domain due to stronger segregation of the two constituting chains. Likewise, the value of $\Delta a/\langle a \rangle$ decreased with increasing C.

We can attribute this variation to the variation of the number of formed domains per unit volume, $\langle n \rangle$. As a bcc lattice consists of two spheres in one unit cell, $\langle n \rangle$, is given from $\langle a \rangle$ using eq 9 as shown in Figure 8a. Interestingly, $\langle n \rangle$ is rather invariant irrespective of f_w. This means that the number of domains is predetermined when the polymer concentration is fixed. The association number, i.e., the number of polymer chains per spherical domain, N_{assoc} can be evaluated via the following equation,

$$N_{assoc} = \frac{f_{pPhOVE} V_{domain} d_{domain}}{M_{pPhOVE}} N_A \quad (12)$$

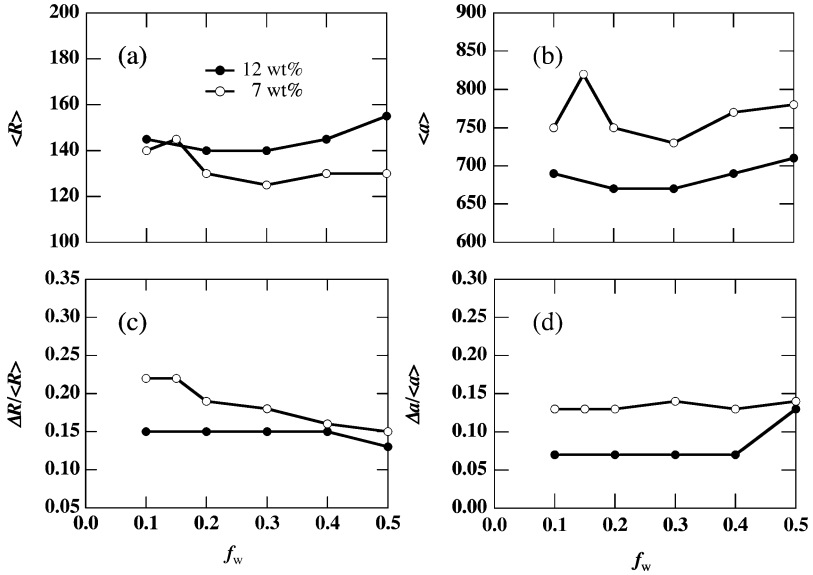

Figure 7. Variations of the structure parameters (a) R, (b) a, (c) $\Delta R/R$, and (d) $\Delta a/a$, evaluated by curve fitting.

where f_{pPhOVE}, V_{domain}, M_{pPhOVE}, and d_{domain} are the volume fraction of pPhOVE, the volume of the spherical domain, the molecular weight of pPhOVE and the mass density of the spherical domain, respectively, and N_A is Avogadro's number. Here, we assumed $d_{domain} = 1.0$ g/cm^3 for simplicity. The variable f_{pPhOVE} is the pPhOVE volume fraction in the spherical domain given by

$$f_{pPhOVE} = \frac{(\rho - \rho_{solv})f_{pMOVE} - \sqrt{\dfrac{I(0)_{obs}\langle a\rangle^3}{2V_{domain}^2}}}{(\rho_{pPhOVE} - \rho_{solv})} \qquad (13)$$

Parts b and c of Figure 8 show the variations of N_{assoc} and f_{pPhOVE} with f_w for the cases of 7 and 12 wt %. N_{assoc} increases with f_w because f_{pPhOVE} increases with f_w as shown in Figure 8c. The increase of f_{pPhOVE} with f_w is due to the fact that the initial polymer concentration in acetone, C_0, was different. The higher the f_w, the higher C_0, resulting in an association with a larger number of polymer chains after water addition. Then, the solvent in the pPhOVE domains is squeezed out by increasing f_w by keeping N_{assoc} determined at the onset of phase separation.

As mentioned above, it was shown that the polymer chains are assembled into spherical microdomains packed in a bcc style after addition of moderate amount of water. This formation of microphase-separated structure is the origin of the phenomenological sol−gel transition shown in Figure 2. In the next section, we will examine the architecture of the microphase separation.

4. Architecture of the Microphase Separation in the Gel State. We first propose two models for the spatial variations in scattering length density as shown in Figure 9. Model (a) is a spherical domain structure with pPhOVE, and model (b) is vice versa with pMOVE. In the case of model (a), added water molecules are dispersed into acetone matrix, and the solvent becomes poorer. This results in formation of a hydrophobic pPhOVE domain by excluding pMOVE chains and the solvent. In model (b), on the other hand, the added water molecules are trapped into the domain with rather hydrophilic pMOVE chains to prevent the unfavorable

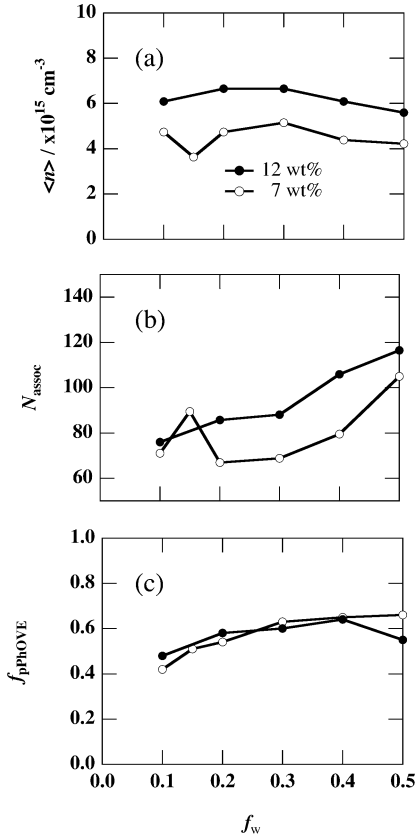

Figure 8. Variations of the structure parameters (a) $\langle n\rangle$, (b) N_{assoc}, and (c) f_{pPhOVE}.

water−pPhOVE interaction. We examined these two models by using a contrast variation method.

As is given by eqs 2 and 3, $I(q)$ is proportional to the square of the scattering length densities between the particles and the matrix:

$$I(q)_{obs} \sim \Delta\rho^2 = (\rho_{matrix} - \rho_{core})^2 \qquad (14)$$

In this experiment, we employed H_2O instead of D_2O as adding solvent to change the contrast of ρ between the matrix and the domain to trace the water molecules after the addition. As the value of ρ for H_2O is negative

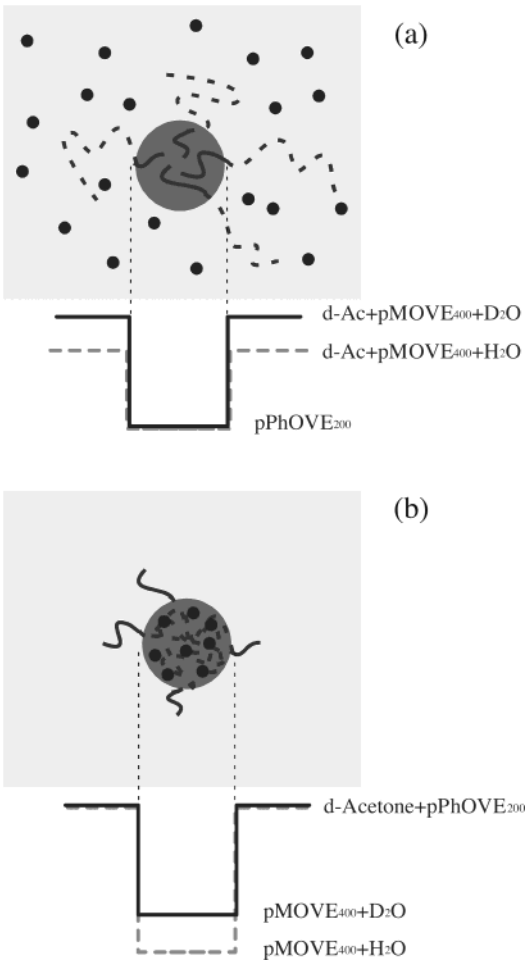

Figure 9. Models and the scattering-length density profiles of a pPhOVE−pMOVE spherical domain.

and those of the others are all positive, H_2O acts to lower the ρ value of its surroundings.

The ratio of the scattering intensities between the H and D systems is given by

$$I(q)_{\text{calc\_H}}/I(q)_{\text{calc\_D}} = \frac{([(\rho_{\text{pMOVE}} - \rho_{\text{solv\_H}})f_{\text{pMOVE}} - (\rho_{\text{pPhOVE}} - \rho_{\text{solv\_H}})f_{\text{pPhOVE}}])^2}{([(\rho_{\text{pMOVE}} - \rho_{\text{solv\_D}})f_{\text{pMOVE}} - (\rho_{\text{pPhOVE}} - \rho_{\text{solv\_D}})f_{\text{pPhOVE}}])^2} \quad (15)$$

where ρ_i and f_i are the scattering length density and the volume fraction of i (=pPhOVE or pMOVE) in the respective domain/matrix. The calculated values of ρ's of polymer chains and mixed D/H-solvents of $f_w = 0.1$ are as follows: $\rho_{\text{pMOVE}} = 0.439 \times 10^{10}$, $\rho_{\text{pPhOVE}} = 1.217 \times 10^{10}$, $\rho_{\text{solv\_H}} = 4.86 \times 10^{10}$, and $\rho_{\text{solv\_D}} = 5.54 \times 10^{10}$ cm^{-2}. In the case of $C = 7$ wt %, the values of $f_{\text{pMOVE}} = 0.036$ and $f_{\text{pPhOVE}} = 0.42$ and the ratio of $I(q)$s were evaluated to be 0.7. In Figure 10, we show the result of the experiment in the sample where $C = 7$ wt % with $f_w = 0.1$. We superimposed the calculated $I(q)$, obtained by multiplying $I(q)$ with the ratio, showing good agreement with the experimental result. As shown in the figure, we obtained a similar shape profile with a decrease in the scattering intensity. This means that the shapes of the formed microphase structures are the same and only the difference in ρ_{matrix} and ρ_{core} has been changed by H/D substitution. Considering the decrease in the intensity, we conclude that the domains are formed with pPhOVE chains as shown in Figure 9a.

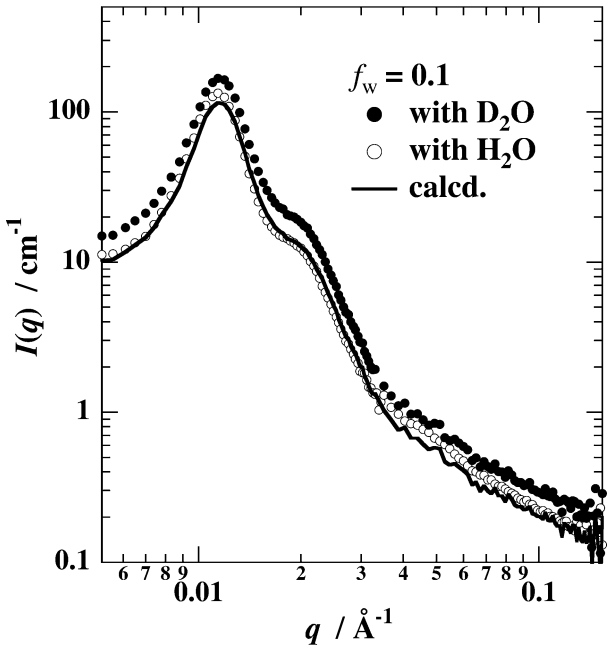

Figure 10. SANS results of the contrast variation experiment for pPhOVE−pMOVE/acetone/water solution with $C = 7$ wt % and $f_w = 0.1$.

5. Comparison of the Heat-Induced and the Water-Induced Phase Separation. In one of the previous papers,[23] we discussed a heat-induced phase separation in poly(2-ethoxyethyl vinyl ether)-*block*-poly(2-hydroxyethyl vinyl ether) (pEOVE−pHOVE) aqueous solutions. In the case of pEOVE−pHOVE, a micelle formation undergoes first, followed by rearrangement to a bcc packed structure. We also studied phase separation of poly(2-ethoxyethyl vinyl ether)-*block*-poly(2-methoxyethyl vinyl ether) (pEOVE−pMOVE) aqueous solutions and found that this system also undergoes heat-induced phase separation. In both cases, pEOVE becomes nonsoluble to water above 20 °C. The difference between the water-induced phase separation studied here in pPhOVE−pMOVE/acetone/water and the heat-induced phase separation observed in pEOVE−pMOVE and pEOVE−pHOVE are due to the nature of environmental sensitivity of the pPhOVE (nonsoluble group to water) and pEOVE (temperature-sensitive). Interestingly enough, we found that the evolutions of microphase separation are different between the two systems.

In Figure 11, we show series of SANS profiles for (a) 20 wt % pEOVE−pMOVE aq solution with increasing T and (b) 12 wt % pPhOVE−pMOVE/acetone/water varying f_w. The thin and thick allows indicate the scattering peaks from the spherical domains and from the ordering of the domains, respectively. As shown in the figure, these two solutions show different responses to the external stimuli, i.e., (a) temperature increase (heat-induced transition) and (b) water addition (solvent-induced transition). The pEOVE−pMOVE system first forms micelles (indicated with the thick arrows) followed by packing of the micelles on increasing temperature (thin arrows). On the other hand, the pPhOVE−pMOVE keeps spatial ordering irrespective of f_w (thick arrows) before pPhOVE domain formation (thin arrows). These differences may be ascribed to the differences in the nature of molecular interactions associated in the mi-

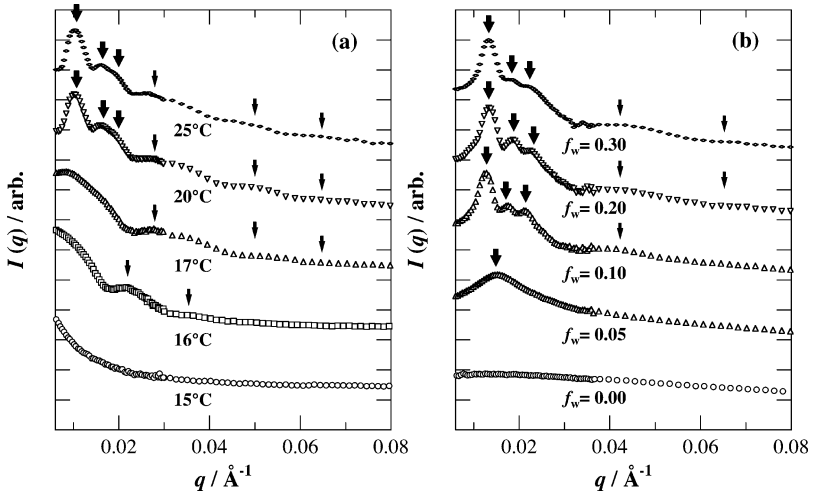

Figure 11. Variations of $I(q)$s for (a) 20 wt % pEOVE−pMOVE aqueous solution (heat-induced microphase-separated structure) with T and (b) 12 wt % pPhOVE−pMOVE/acetone/water solution (water-induced microphase-separated structure) with the fraction of water added to the solution, f_w.

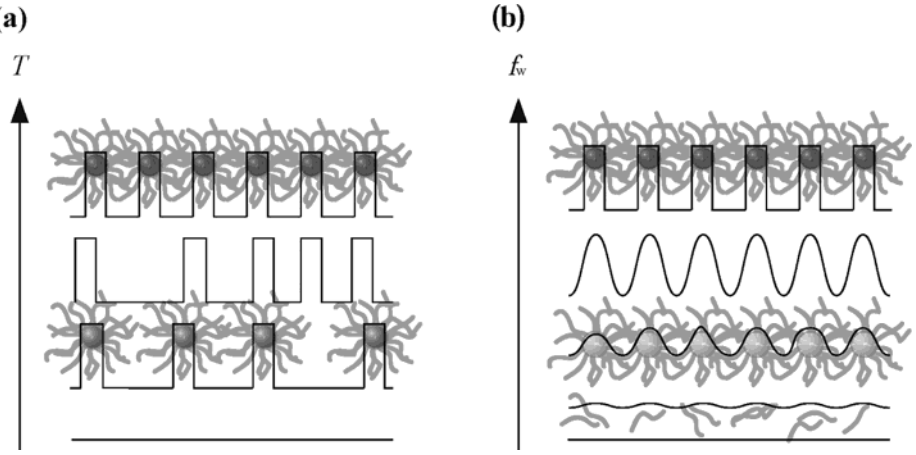

Figure 12. Schematic representations showing the difference in the growth of microphase-separated structure for (a) heat-induced and (b) water-induced phase separations.

crophase separation, i.e., hydrophobic interaction (heat-induced transition) and van der Waals interaction (solvent-induced transition). In the case of the former, the interaction parameter, χ, changes stepwise change near the transition temperature. Poly(*N*-isopropylacrylamide) in water is a typical system, in which χ, changes discretely as was reported by Hirotsu.[29] In this case, the lower critical solution temperature (LCST) of pEOVE in water is about 20 °C. By approaching this temperature, micelles (i.e., microdomains) consisting of pEOVE chains are formed, which is followed by packing to a bcc by further increase in temperature. On the other hand, in the case of solvent-induced microphase separation, χ increases monotonically with f_w resulting in amplification of the concentration fluctuations to form a microphase-separated structure.

Figure 12 illustrates the difference in the evolution processes of the structures by (a) heat-induced and (b) water-induced microphase separations. In the case of part a, micelles with pEOVE chains are formed, followed by rearranging to a bcc packing as was reported elsewhere.[23] This results in a physical gelation. On the other hand, in the case of part b, an amplification of concentration fluctuations takes place due to an increase in χ. Hence, the long spacing of the microdomain structure is fixed in advance to the formation of domains. This type of evolution process in concentration fluctuations is analogous to the spinodal decomposition. Further analyses along this aspect are in progress.

Conclusion

The microphase-separated structure of the pPhOVE−pMOVE/acetone/water was investigated by SANS. The following facts were revealed: (1) By adding water, microphase-separated structures consisting of spherical domains aligned in a bcc style is formed. (2) The structure parameters are around $\langle R\rangle = 130$ Å with $\langle a\rangle = 790$ Å and $\langle R\rangle = 140$Å with $\langle a\rangle = 650$ Å respectively for $C = 7$ and 12 wt %. (3) By the contrast changing experiment, it is confirmed that the spherical domains are constructed with pPhOVE chains. (4) The mechanisms of microphase separations are different between the heat-induced and water-induced microphase separations. The former is initiated by micelle formation followed by rearrangement to a bcc packing, and the latter is an amplification process similar to spinodal decomposition by keeping the long period correlation. Finally, it should be noted that these sharp environmental-sensitive microphase separation could be achieved with a tailor-made block copolymer carrying environment-sensitive functional groups, i.e., ether moiety in this case, in addition to a narrow molecular weight distribution.

Acknowledgment. This work is partially supported by the Ministry of Education, Science, Sports and Culture, Japan (Grant-in-Aid, and 14350493, 14045216 to M.S.). The SANS experiment was performed with the approval of Institute for Solid State Physics, The University of Tokyo (Proposal No. 03-3502), at Japan Atomic Energy Research Institute, Tokai, Japan.

References and Notes

(1) Molau, G. E. In *Block Polymers*; Aggarwal, S. L., Ed.; Plenum Press: New York, 1970.
(2) Helfand, E.; Wasserman, Z. R. *Macromolecules* **1976**, *9*, 879.
(3) Helfand, E.; Wasserman, Z. R. In *Developments in Block Copolymers*; Goodman, I., Ed.; Applied Science: New York, 1982.
(4) Hamley, I. W. *The Physics of Block Copolymers*; Oxford University Press: Oxford, England, 1998.
(5) Helfand, E.; Wasserman, Z. R. *Macromolecules* **1978**, *11*, 960.
(6) Stanley, H. E. *Introduction to Phase Transition and Critical Phenomena*; Oxford University Press: New York, 1971.
(7) Hashimoto, T. In *Thermoplastic Elastomers*; Holden, G., Legge, N. R., Qurik, R. P., Schroeder, H. E., Eds.; Hanser: Munich, Germany, 1996; p 460.
(8) Watanabe, H.; Kotaka, T.; Hashimoto, T.; Shibayama, M.; Kawai, H. *J. Rheol.* **1982**, *26*, 153.
(9) Hashimoto, T.; Shibayama, M.; Kawai, H.; Watanabe, H.; Kotaka, T. *Macromolecules* **1983**, *16*, 361.
(10) Hashimoto, T.; Shibayama, M.; Kawai, H. *Macromolecules* **1983**, *16*, 1093.
(11) Shibayama, M.; Hashimoto, T.; Kawai, H. *Macromolecules* **1983**, *16*, 16.
(12) McConnell, G. A.; Gast, A. P.; Huang, J. S.; Smith, S. D. *Phys. Rev. Lett.* **1993**, *71*, 2102.
(13) Mortensen, K. *Prog. Colloid Polym. Sci.* **1993**, *91*, 69.
(14) Mortensen, K.; Brown, W. *Macromolecules* **1993**, *26*, 4128.
(15) Wanka, G.; Hoffman, H.; lbricht, W. *Macromolecules* **1994**, *27*, 4145.
(16) Alexandridis, P.; Hatton, T. A. *Colloids Surf. A* **1995**, *96*, 1.
(17) Aoshima, S.; Hashimoto, K. *J. Polym. Sci., Part A: Polym. Chem.* **2001**, *39*, 746.
(18) Sugihara, S.; Hashimoto, K.; Matsumoto, Y.; Kanaoka, S.; Aoshima, S. *J. Polym. Sci., Part A: Polym. Chem.* **2003**, *41*, 3300.
(19) Aoshima, S.; Sugihara, S. *J. Polym. Sci., Part A: Polym. Chem.* **2000**, *38*, 3962.
(20) Sugihara, S.; Aoshima, S. *Koubunshi Ronbunshu* **2001**, *58*, 304.
(21) Sugihara, S.; Matsuzono, S.; Sakai, H.; Abe, M.; Aoshima, S. *J. Polym. Sci., Part A: Polym. Chem.* **2001**, *39*, 3190.
(22) Aoshima, S.; Oda, H.; Kobayashi, E. *J. Polym. Sci., Part A: Polym. Chem.* **1992**, *30*, 2407.
(23) Okabe, S.; Sugihara, S.; Aoshima, S.; Shibayama, M. *Macromolecules* **2002**, *35*, 8139.
(24) Hosemann, R.; Bagchi, S. N. *Direct Analysis of Diffraction by Matter*; North-Holland: Amsterdam, 1962.
(25) Matsuoka, H.; Tanaka, H.; Hashimoto, T.; Ise, N. *Phys. Rev. B* **1987**, *36*, 1754.
(26) Matsuoka, H.; Tanaka, H.; Iizuka, N.; Hashimoto, T.; Ise, N. *Phys. Rev. B* **1990**, *41*, 3854.
(27) Shibayama, M.; Okabe, S.; Nagao, M.; Sugihara, S.; Aoshima, S.; Harada, T.; Matsuoka, H. *Macromol. Res.* **2002**, *44*, 311.
(28) Hashimoto, H.; Fujimura, M.; Hashimoto, T.; Kawai, H. *Macromolecules* **1981**, *14*, 844.
(29) Hirotsu, S. *J. Chem. Phys.* **1991**, *94*, 3949.

MA0495442